

SELECTED TOPICS IN APPLIED PHYSICS

Fabrication of high-qualified  $(\text{Bi}_{1-x}\text{Ba}_x)\text{FeO}_3$   
multiferroic thin films by using a pulsed DC  
reactive sputtering method and demonstration of  
magnetization reversal by electric field

To cite this article: Satoru Yoshimura and Munusamy Kuppan 2018 *Jpn. J. Appl. Phys.* **57** 0902B7

View the [article online](#) for updates and enhancements.

You may also like

- [Defect Chemistry and Phase Equilibria of  \$\(\text{La}\_{1-x}\text{Ca}\_x\)\text{FeO}\_3\$ : Thermodynamic Modeling](#)  
Sung Hoon Lee, Venkateswara Rao  
Manga, Michael F. Carolan et al.
- [Synthesis and characterization of coprecipitation-prepared La-doped  \$\text{BiFeO}\_3\$  nanopowders and their bulk dielectric properties](#)  
Benjaporn Yotburut, Teerapon Yamwong,  
Prasit Thongbai et al.
- [Structural, optical and magnetic properties of  \$\text{Sm}^{3+}\$  doped yttrium orthoferrite \( \$\text{YFeO}\_3\$ \) obtained by sol-gel synthesis route](#)  
P S J Bharadwaj, Swarup Kundu, Vijay Sai  
Kollipara et al.



# Fabrication of high-qualified $(\text{Bi}_{1-x}\text{Ba}_x)\text{FeO}_3$ multiferroic thin films by using a pulsed DC reactive sputtering method and demonstration of magnetization reversal by electric field

Satoru Yoshimura<sup>1,2\*</sup> and Munusamy Kuppan<sup>3</sup>

<sup>1</sup>Research Center for Engineering Science, Graduate School of Engineering Science, Akita University, Akita 010-8502, Japan

<sup>2</sup>PRESTO, Japan Science and Technology Agency (JST), Kawaguchi, Saitama 332-0012, Japan

<sup>3</sup>Regional Innovation Center, Akita University, Akita 010-8502, Japan

\*E-mail: syoshi@gipc.akita-u.ac.jp

Received January 15, 2018; revised March 1, 2018; accepted March 17, 2018; published online June 26, 2018

$(\text{Bi}_{1-x}\text{Ba}_x)\text{FeO}_3$  multiferroic thin films with ferromagnetism and ferroelectricity were fabricated by a pulsed DC reactive sputtering and applied to create a magnetic domain using an electric field. The (001)-oriented  $(\text{Bi}_{1-x}\text{Ba}_x)\text{FeO}_3$  thin films, the electric polarization direction of which is perpendicular to the film plane, were fabricated onto a non-single-crystalline substrate with a Ta seedlayer/(111)-oriented Pt underlayer. A low pulse frequency (long time for sputtering OFF) and a high sputtering power (high-energy deposition) were effective for the acceleration of the crystallization of the  $(\text{Bi}_{1-x}\text{Ba}_x)\text{FeO}_3$  phase owing to the enhancement of the surface diffusion of sputtered atoms on the substrate surface. The saturation magnetization of the film was approximately  $90 \text{ emu/cm}^3$  and the coercivity was approximately 2.5 kOe. Magnetic force microscopy analysis of the  $(\text{Bi}_{0.48}\text{Ba}_{0.52})\text{FeO}_3$  film confirmed that the magnetization was generated by applying only a local electric field. The multiferroic film described here is expected to be useful for electric-field-driven magnetic devices. © 2018 The Japan Society of Applied Physics

## 1. Introduction

Magnetization reversal by an electric field is a prospective technology for future magnetic devices owing to its low power consumption and easy operation for magnetization reversal. For example, in the case of magnetic recording devices such as hard-disk drives (HDDs), magnetic field writing will gradually become more difficult owing to the increase in the required magnetic field. This is because the switching magnetic field of recorded bits (coercivity of magnetic grains) increases to inhibit the thermal agitation of magnetization. Therefore, recently, energy-assisted magnetic recording technologies for next-generation HDDs such as thermally assisted magnetic recording<sup>1-3</sup> and microwave-assisted magnetic recording<sup>4-6</sup> have been widely studied to decrease the switching magnetic field. However, the energy-assisted magnetic recording technologies also consume large quantities of power and the structure of the magnetic field writing head is complicated owing to additional elements such as a plasmon antenna for thermally assisted magnetic recording or a spin torque oscillator for microwave assisted-magnetic recording. Therefore, a new technique for magnetization reversal is needed, and the electric field writing can be used for magnetic recording devices with multiferroic thin films. The power requirement for switching the magnetization direction by this process is very low, the structure of the writing element is simple (involving a needle-shaped conductive element), and a very high electric field can be easily applied to the multiferroic layer because it is thin.

Several techniques of controlling the magnetization by applying an electric field were reported. (1) The control of magnetization direction by applying an electric field was performed in piezoelectric and magnetostrictive laminate composites<sup>7,8</sup> or multilayer structures.<sup>9,10</sup> (2) The control of the magnetic anisotropy of a thin metallic magnetic layer by applying an electric field was performed in magnetic tunnel junctions with trilayers of thin metallic magnetic layer/thin insulating layer/metallic magnetic layer.<sup>11-13</sup> (3) The reversal of the magnetization direction of a thin metallic magnetic

layer by applying an electric field was performed in a bilayer with  $\alpha\text{-Cr}_2\text{O}_3$  (dielectric property and antiferromagnetic property)/thin magnetic layer.<sup>14,15</sup> (4) The reversal of the magnetization direction of a thin metallic magnetic layer by applying an electric field was performed in a bilayer with  $\text{BiFeO}_3$  (high ferroelectric Curie temperature of 1120 K and high antiferromagnetic Néel temperature of 640 K)/thin magnetic layer.<sup>16-18</sup> (5) The reversal of the magnetization directions of  $(\text{Dy,Tb})\text{FeO}_3$ ,<sup>19</sup>  $\text{SmFeO}_3$ ,<sup>20</sup> and  $\text{YbFeO}_3$ <sup>21</sup> (ferromagnetism and ferroelectricity at low temperature) by applying an electric field was performed. However, there are problems regarding magnetic device application in these systems. Complete magnetization reversal is difficult in system 1, both the electric field and the magnetic field are needed for magnetization reversal in systems 2 and 3, only a thin magnetic layer is effective for magnetization reversal in systems 2, 3, and 4, and only a very low temperature is effective for magnetization reversal in system 5. Therefore, a new system that can complete the magnetization reversal in a single phase (single layer) with ferromagnetism and ferroelectricity with a high Curie temperature is needed.

These days, suitable multiferroic materials such as  $(\text{Bi}_{1-x}\text{Ba}_x)\text{FeO}_3$ ,<sup>22</sup>  $(\text{Bi}_{1-x}\text{Ba}_x)(\text{Fe}_{1-y}\text{Ti}_y)\text{O}_3$ ,<sup>23</sup>  $\text{Ba}(\text{Ti}_{1-x}\text{Fe}_x)\text{O}_3$ ,<sup>24</sup> and  $\text{Bi}(\text{Fe}_{1-x}\text{Co}_x)\text{O}_3$ <sup>25,26</sup> with ferromagnetism and ferroelectricity at room temperature are reported. In a previous study, we fabricated Ta seedlayer/(111)-oriented Pt underlayer/(001)-oriented  $(\text{Bi}_{1-x}\text{Ba}_x)\text{FeO}_3$  multiferroic thin films with electric polarization perpendicular to the film plane onto a thermally oxidized Si wafer using an ultrahigh-vacuum (UHV) sputtering system.<sup>27</sup> Very high frequency (VHF) (40.68 MHz) plasma irradiation with an electric power of 5 W was applied during the radio-frequency (RF) (13.56 MHz) sputter deposition<sup>28</sup> of the  $(\text{Bi}_{1-x}\text{Ba}_x)\text{FeO}_3$  film. The  $(\text{Bi}_{0.6}\text{Ba}_{0.4})\text{FeO}_3$  film, in which the Ba concentration was optimized, exhibited hysteresis curves indicating ferromagnetic and ferroelectric behavior and had a saturation magnetization of about  $60 \text{ emu/cm}^3$ , a coercivity of about 2.5 kOe, and a high Curie temperature of about 400 °C. Magnetic force microscopy (MFM) analysis of the  $(\text{Bi}_{0.6}\text{Ba}_{0.4})\text{FeO}_3$  film

confirmed that the magnetization was reversed by applying only a local electric field.<sup>27</sup> This indicates that the magnetization direction in the  $(\text{Bi}_{0.6}\text{Ba}_{0.4})\text{FeO}_3$  film could be controlled on the micrometer scale by simply applying an electric field. However, the saturation magnetization and insulation of the films were insufficient for high-performance magnetic device application.

Here, a pulsed DC reactive sputtering technique was reported as a useful fabrication method of oxide or nitride films from the viewpoints of high deposition rate, high sputtering voltage, free arcs, and removal of charges on the surface of a sputtering target.<sup>29</sup> Moreover, this fabrication method is also effective for the enhancement of the surface diffusion of sputtered atoms on the substrate surface by high-energy deposition with time interval. In this study, we fabricated high-qualified  $(\text{Bi}_{1-x}\text{Ba}_x)\text{FeO}_3$  thin films by reactive pulsed DC sputtering. We also demonstrated the control of the magnetization direction on the micrometer scale by applying a local electric field on a scanning probe microscope (SPM) with a Co–Zr–Nb-coated conductive tip.

## 2. Experimental methods

Multilayers of Ta (5 nm)/Pt (100 nm)/ $(\text{Bi}_{1-x}\text{Ba}_x)\text{FeO}_3$  (300 nm) were deposited onto a thermally oxidized Si wafer using a UHV sputtering system. The Ba concentration  $x$  was varied from 0.30 to 0.75. The Ta seedlayer, Pt underlayer, and  $(\text{Bi}_{1-x}\text{Ba}_x)\text{FeO}_3$  layer were deposited at room temperature, 300 °C, and 570 °C, respectively. The film thickness and deposition temperature of the Ta seedlayer and Pt underlayer were optimized to obtain a strong (111) orientation of the Pt underlayer.<sup>30</sup> The VHF (40.68 MHz) plasma irradiation<sup>28</sup> during the reactive pulsed DC sputtering deposition of  $(\text{Bi}_{1-x}\text{Ba}_x)\text{FeO}_3$  films was performed with an electric power of 5 W to obtain the crystal grain growth of  $(\text{Bi}_{1-x}\text{Ba}_x)\text{FeO}_3$  thin films. The frequency of pulsed DC was varied from 50 to 250 kHz. Here, the duty ratios between sputtering ON and OFF are about 2–3 and 1, for example, the time of sputtering ON is 15  $\mu\text{s}$  and that of OFF is 5  $\mu\text{s}$  for 50 kHz, and the time of sputtering ON is 2.6  $\mu\text{s}$  and that of OFF is 1.4  $\mu\text{s}$  for 250 kHz. The sputtering power of pulsed DC was varied from 100 to 200 W. The composition of the fabricated  $(\text{Bi}_{1-x}\text{Ba}_x)\text{FeO}_3$  films was analyzed by energy dispersive X-ray spectroscopy (EDS). The crystallographic orientations and crystalline structures of the fabricated  $(\text{Bi}_{1-x}\text{Ba}_x)\text{FeO}_3$  films were analyzed by X-ray diffraction (XRD) analysis. The magnetization curves of  $(\text{Bi}_{1-x}\text{Ba}_x)\text{FeO}_3$  films were measured using a vibrating sample magnetometer (VSM) with the application of a magnetic field parallel to the film surface. The ferroelectric hysteresis loops of the  $(\text{Bi}_{1-x}\text{Ba}_x)\text{FeO}_3$  films were measured using a ferroelectric tester. The local electric field was applied to the  $(\text{Bi}_{1-x}\text{Ba}_x)\text{FeO}_3$  film using an SPM with a conductive, magnetic Co–Zr–Nb tip. The electric and magnetic domain structures of the  $(\text{Bi}_{1-x}\text{Ba}_x)\text{FeO}_3$  film were analyzed by electric force microscopy (EFM) and magnetic force microscopy (MFM), respectively, with a conductive, magnetic Co–Zr–Nb tip.

## 3. Results and discussion

Figure 1 shows the XRD profiles of the Bi–Ba–Fe–O films fabricated with various Ba concentrations on a thermally oxidized Si substrate with a Ta/Pt layer. The profiles are dif-

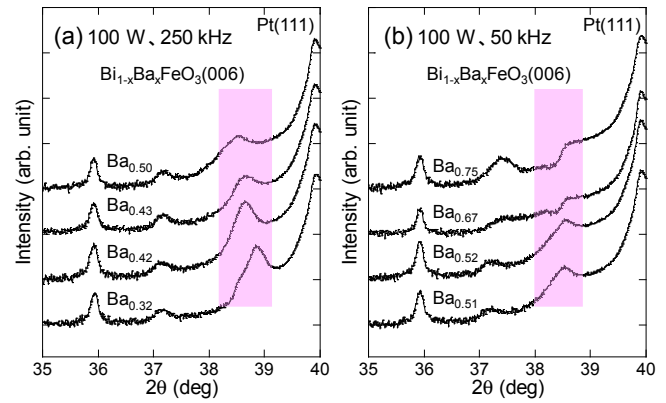


**Fig. 1.** (Color online) XRD profiles of Ta seedlayer/Pt underlayer and Bi–Ba–Fe–O films on Ta/Pt layer fabricated with various Ba concentrations [pulsed DC frequencies of (a) 250 and (b) 50 kHz].

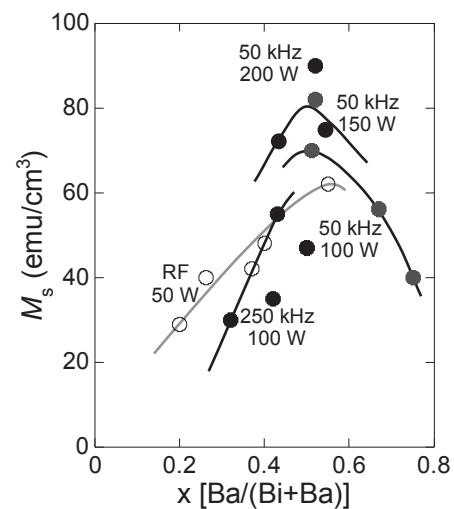


**Fig. 2.** Dependence of saturation magnetization on Ba concentration in Bi–Ba–Fe–O films fabricated by pulsed DC reactive sputtering with various fabrication conditions and RF sputtering.

ferentiated by fabrication condition of pulsed DC frequency [(a) 250 kHz and (b) 50 kHz], because the pulsed DC frequency affects film quality, as described below. The Pt underlayer was found to have a strong (111) orientation and the full width at half maximum of the rocking curve for the Pt(111) diffraction was 2.0°. The Bi–Ba–Fe–O films with the Ba concentration of less than 0.55 were found to have a strong (006) peak; this indicates that these films have a (001) orientation. Here, the peak at around 35.8° is from the substrate, and the peak at around 37.2° is from the impurity phase or second phase (unknown phase) with a very small quantity. With increasing Ba concentration, the (006) peak shifts to a lower angle [Fig. 1(a)]. This indicates that the Bi atoms of the  $\text{BiFeO}_3$  phase are replaced by Ba atoms. On the other hand, in the case of Bi–Ba–Fe–O films with a Ba concentration of more than 0.6, the (006) peak disappears [Fig. 1(b)] and other peaks appear (not shown). This indicates that the formation of the  $\text{BiFeO}_3$  phase is hindered by an excess amount of Ba. These results indicate that the  $(\text{Bi}_{1-x}\text{Ba}_x)\text{FeO}_3$  films with  $x < 0.6$  can be formed with a single phase.

Figure 2 shows the dependence of the saturation magnetization  $M_s$  on the Ba concentration in the Bi–Ba–Fe–O films fabricated by pulsed DC reactive sputtering. The dependence

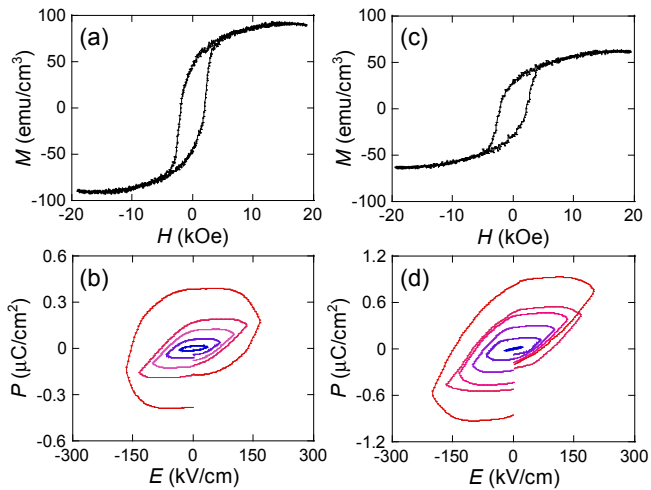


**Fig. 3.** (Color online) Magnetization curves (a, c) and ferroelectric curves (b, d) of  $(\text{Bi}_{1-x}\text{Ba}_x)\text{FeO}_3$  ( $x \sim 0.5$ ) films fabricated by pulsed DC reactive sputtering (a, b) and RF sputtering (c, d).

of  $M_s$  on the Ba concentration in the Bi–Ba–Fe–O films fabricated by RF sputtering is also shown for comparison in this figure. The sputtering power is changed in the case of Bi–Ba–Fe–O films fabricated by the pulsed DC reactive sputtering, and the sputtering power is optimized in the case of Bi–Ba–Fe–O films fabricated by RF sputtering. With increasing Ba concentration up to around 0.5,  $M_s$  increased in both Bi–Ba–Fe–O films fabricated by the pulsed DC reactive and RF sputterings. This is due to the transformation from the antiferromagnetic phase to the ferrimagnetic phase.<sup>22)</sup> The decrease in  $M_s$  in the Bi–Ba–Fe–O films with the Ba concentration of more than 0.6 is due to the inhibition of the formation of the  $(\text{Bi}_{1-x}\text{Ba}_x)\text{FeO}_3$  phase, as mentioned in Fig. 1. In the case of  $(\text{Bi}_{1-x}\text{Ba}_x)\text{FeO}_3$  films with the Ba concentration of about 0.5 fabricated by the pulsed DC reactive sputtering,  $M_s$  increases from 70 to 90  $\text{emu}/\text{cm}^3$  with increasing sputtering power. The  $M_s$  of 90  $\text{emu}/\text{cm}^3$  was 1.5 times larger than that of the  $(\text{Bi}_{1-x}\text{Ba}_x)\text{FeO}_3$  film with the Ba concentration of about 0.5 fabricated by the RF sputtering.

Figure 3 shows the in-plane magnetization curves (a), (c) and ferroelectric curves (b), (d) of the  $(\text{Bi}_{1-x}\text{Ba}_x)\text{FeO}_3$  ( $x \sim 0.5$ ) films fabricated by the pulsed DC reactive sputtering (a), (b) and RF sputtering (c), (d). A clear hysteresis loop in both magnetization and ferroelectric curves was observed. The  $M_s$  of the  $(\text{Bi}_{1-x}\text{Ba}_x)\text{FeO}_3$  film fabricated by the pulsed DC reactive sputtering was 1.5 times larger than that of the film fabricated by the RF sputtering, as mentioned before. The coercivity of magnetization curves was around 2 kOe, and the squareness  $S$  (= remanent magnetization  $M_r/M_s$ ) was around 0.60. On the other hand, the coercivity and  $S$  with the out-of-plane direction of the film were 1.5 kOe and 0.40 (not shown), respectively. This indicates that this film has somewhat perpendicular magnetic anisotropy. These magnetic properties are available for magnetic devices. For the measurement of ferroelectric curves, the maximum electric field was about 200 kV/cm due to the insulating destruction. The hysteresis of the  $(\text{Bi}_{1-x}\text{Ba}_x)\text{FeO}_3$  film fabricated by the pulsed DC reactive sputtering was clearer than that of the film fabricated by the RF sputtering. The electric current at 5 V application for the  $(\text{Bi}_{1-x}\text{Ba}_x)\text{FeO}_3$  film fabricated by the pulsed DC reactive sputtering was 300 nA, which is 5 times smaller than that in

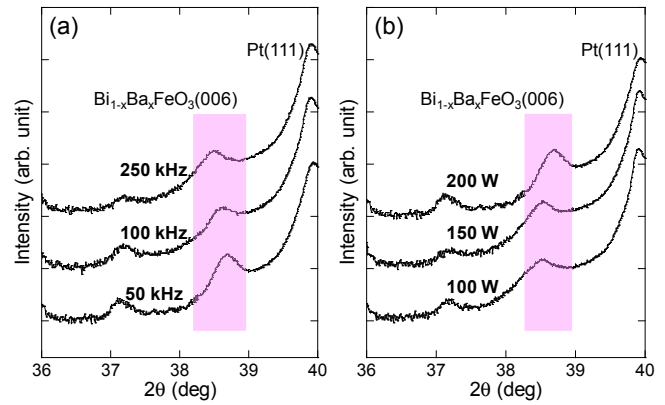


**Fig. 4.** (Color online) XRD profiles of  $(\text{Bi}_{1-x}\text{Ba}_x)\text{FeO}_3$  ( $x \sim 0.5$ ) films fabricated by pulsed DC reactive sputtering with various pulsed frequencies (a) and sputtering powers (b).

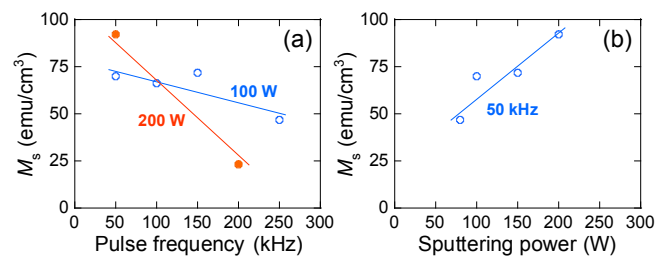


**Fig. 5.** (Color online) Dependence of saturation magnetization on pulsed frequency (a) and sputtering power (b) in  $(\text{Bi}_{1-x}\text{Ba}_x)\text{FeO}_3$  ( $x \sim 0.5$ ) films fabricated by pulsed DC reactive sputtering.

the case of the RF sputtering. These indicate that the use of the pulsed DC reactive sputtering is the key to obtaining high-qualified  $(\text{Bi}_{1-x}\text{Ba}_x)\text{FeO}_3$  multiferroic films. The relationship between the magnetic and ferroelectric properties will be discussed in a future study because only the minor loop of the electric property was measured here.

Figure 4 show the XRD profiles of the  $(\text{Bi}_{1-x}\text{Ba}_x)\text{FeO}_3$  ( $x \sim 0.5$ ) films fabricated by the pulsed DC reactive sputtering with various pulsed frequencies (a) and sputtering powers (b). As the pulsed frequencies are decreased and the sputtering powers are increased, the  $(\text{Bi}_{1-x}\text{Ba}_x)\text{FeO}_3$  (006) peak intensity increased. [This is considered to accelerate the crystallization of the  $(\text{Bi}_{1-x}\text{Ba}_x)\text{FeO}_3$  phase.] Figure 5 shows the dependences of  $M_s$  on the pulsed frequency (a) and sputtering power (b) in the  $(\text{Bi}_{1-x}\text{Ba}_x)\text{FeO}_3$  ( $x \sim 0.5$ ) films fabricated by the pulsed DC reactive sputtering. As the pulsed frequencies are decreased and the sputtering powers are increased,  $M_s$  increased. This is due to the acceleration of the crystallization, as mentioned in Fig. 4. (The reason for the acceleration of the crystallization is considered to be the enhancement of the surface diffusion of sputtered atoms on the substrate surface by high-energy deposition with a long time interval.)

Figures 6(a)–6(d) show topographic, MFM (tip end: N), EFM (tip end: +), and EFM (tip end: –) images, respectively, of the  $(\text{Bi}_{0.48}\text{Ba}_{0.52})\text{FeO}_3$  film fabricated by the pulsed DC reactive sputtering with the pulsed frequency of 50 kHz and the sputtering power of 200 W after applying a DC voltage of –10 V (333 kV/cm) with  $2 \times 2 \mu\text{m}^2$  to the film. The MFM images were captured with a Co–Zr–Nb magnetic tip that was magnetized to saturation at the end of the tip such that the magnetization direction would be perpendicular to the sample

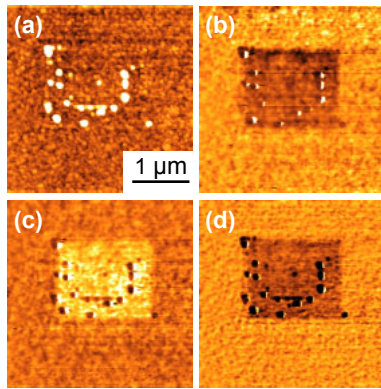


**Fig. 6.** (Color online) (a) Topographic, (b) MFM (tip end: N), (c) EFM (tip end: +), and (d) EFM (tip end: -) images of  $(\text{Bi}_{0.48}\text{Ba}_{0.52})\text{FeO}_3$  film after applying DC voltage of  $-10\text{ V}$  with  $2 \times 2\ \mu\text{m}^2$  to the film.

surface and the direction of the detected magnetic field from the sample would also be vertical to the sample surface. For the EFM imaging, the Pt underlayer was grounded and a DC voltage of  $+1.0\text{ V}$  ( $+33\text{ kV/cm}$ ) or  $-1.0\text{ V}$  ( $-33\text{ kV/cm}$ ) was applied to the Co–Zr–Nb conductive tip. Because this DC electric field was smaller than the coercive electric field of the  $(\text{Bi}_{0.48}\text{Ba}_{0.52})\text{FeO}_3$  film, as depicted in Fig. 3, polarization reversal did not occur during this imaging. In the MFM image obtained with the tip magnetized at the end, an attractive force between the tip and the sample was observed in the ferromagnetic domain structure, indicating that the magnetization direction was downward toward the film surface. In the EFM image obtained with the tip voltage of  $+1.0\text{ V}$ , a repulsive force between the tip and the sample was observed in the ferroelectric domain structure, which indicates a positive electric charge in this area. In an EFM image obtained with a tip voltage of  $-1.0\text{ V}$ , the attractive force between the tip and the sample was observed in the ferroelectric domain structure, which indicates a positive electric charge in this area. These images show that clear micrometer-scale ferroelectric domains were formed upon application of the local electric field. In an MFM image obtained with a tip voltage of  $0\text{ V}$ , the attraction in the area and the surrounding area did not change for both before and after EFM measurements with tip voltages of  $-1.0$  and  $+1.0\text{ V}$  (not shown here). Therefore, it can be concluded that micrometer-scale magnetization was achieved by applying a local electric field and that the directions of  $P$  and  $M$  are parallel. Thus, the proposed multiferroic films are expected to be useful in novel magnetic recording devices driven by electric field writing.

#### 4. Conclusions

In this study, we fabricated high-qualified  $(\text{Bi}_{1-x}\text{Ba}_x)\text{FeO}_3$  multiferroic thin films by using pulsed DC reactive sputtering and demonstrated local magnetization reversal by the application of an electric field. The deposition with high energy with a long time interval is effective for the acceleration of the crystallization of the  $(\text{Bi}_{1-x}\text{Ba}_x)\text{FeO}_3$  phase owing to the enhancement of the surface diffusion of sputtered atoms on the substrate surface. The  $(\text{Bi}_{0.48}\text{Ba}_{0.52})\text{FeO}_3$  film was found to have a high saturation magnetization of about  $90\text{ emu/cm}^3$  and a high coercivity of about  $2\text{ kOe}$ . MFM images revealed that the magnetization direction in the  $(\text{Bi}_{0.48}\text{Ba}_{0.52})\text{FeO}_3$  film could be controlled on a micrometer scale by simply applying

an electric field. From these results, the proposed multiferroic film is expected to be useful for applications in electric field-driven magnetic devices. We are developing equipment for the measurement of the electromagnetic effect ( $M$ – $E$  curve) for multiferroic thin films. We will fabricate the multiferroic thin films with very high insulation and will complete the equipment for the measurement of the electromagnetic effect. Then, we will discuss the relationship between the magnetic and ferroelectric properties of the multiferroic thin films.

#### Acknowledgments

This work was partially supported by the Mazda Foundation, Casio Science Promotion Foundation, and JST/PRESTO (No. JPMJPR152C, ID: 15655293).

- 1) J. U. Thiele, S. Maat, and E. E. Fullerton, *Appl. Phys. Lett.* **82**, 2859 (2003).
- 2) R. E. Rottmayer, S. Batra, D. Buechel, W. A. Challener, J. Hohlfield, Y. Kubota, L. Li, B. Lu, C. Mihalcea, K. Mountfield, K. Pelhos, C. Peng, T. Rausch, M. A. Seigler, D. Weller, and X. M. Yang, *IEEE Trans. Magn.* **42**, 2417 (2006).
- 3) M. H. Kryder, E. C. Gage, T. W. McDaniel, W. A. Challener, R. E. Rottmayer, G. Ju, Y. T. Hsia, and M. F. Erden, *Proc. IEEE* **96**, 1810 (2008).
- 4) J. G. Zhu, X. Zhu, and Y. Tang, *IEEE Trans. Magn.* **44**, 125 (2008).
- 5) Y. Tang and J. G. Zhu, *IEEE Trans. Magn.* **44**, 3376 (2008).
- 6) J. G. Zhu and Y. Wang, *IEEE Trans. Magn.* **46**, 751 (2010).
- 7) J. Ryu, A. V. Carazo, K. Uchino, and H.-E. Kim, *Jpn. J. Appl. Phys.* **40**, 4948 (2001).
- 8) S. Dong, J. F. Li, and D. Viehland, *IEEE Trans. Ultrason. Ferroelectr. Freq. Control* **50**, 1253 (2003).
- 9) M. Avellaneda and G. Harshé, *J. Intell. Mater. Syst. Struct.* **5**, 501 (1994).
- 10) G. Srinivasan, E. Rasmussen, J. Gallegos, R. Srinivasan, Y. Bokhan, and V. Laletin, *Phys. Rev. B* **66**, 029902 (2002).
- 11) M. Weisheit, S. Fähler, A. Marty, Y. Souche, C. Poinson, and D. Givord, *Science* **315**, 349 (2007).
- 12) T. Maruyama, Y. Shiota, T. Nozaki, K. Ohta, N. Toda, M. Mizuguchi, A. Tulapurkar, T. Shinjo, M. Shiraishi, S. Mizukami, Y. Ando, and Y. Suzuki, *Nat. Nanotechnol.* **4**, 158 (2009).
- 13) T. Nozaki, Y. Shiota, M. Shiraishi, T. Shinjo, and Y. Suzuki, *Appl. Phys. Lett.* **96**, 022506 (2010).
- 14) Y. Shiratsuchi, T. Fujita, H. Oikawa, H. Noutomi, and R. Nakatani, *Appl. Phys. Express* **3**, 113001 (2010).
- 15) T. Ashida, M. Oida, N. Shimomura, T. Nozaki, T. Shibata, and M. Shashi, *Appl. Phys. Lett.* **104**, 152409 (2014).
- 16) X. Qi, H. Kim, and M. G. Blamire, *Philos. Mag. Lett.* **87**, 175 (2007).
- 17) Y. Chu, L. Martin, M. Holcomb, M. Gajek, A. Han, Q. He, N. Balke, C. Yang, D. Lee, W. Hu, Q. Zhan, P. Yang, A. Rodriguez, A. Scol, S. Wang, and R. Ramesh, *Nat. Mater.* **7**, 478 (2008).
- 18) K. Sone, H. Naganuma, M. Ito, T. Miyazaki, T. Nakajima, and S. Okamura, *Sci. Rep.* **5**, 9348 (2015).
- 19) Y. Tokunaga, Y. Taguchi, T. Arima, and Y. Tokura, *Nat. Phys.* **8**, 838 (2012).
- 20) J. H. Lee, Y. K. Jeong, J. H. Park, M. A. Oak, H. M. Jang, J. Y. Son, and J. F. Scott, *Phys. Rev. Lett.* **107**, 117201 (2011).
- 21) Y. K. Jeong, J. H. Lee, S. J. Ahn, S. W. Song, H. M. Jang, H. Choi, and J. F. Scott, *J. Am. Chem. Soc.* **134**, 1450 (2012).
- 22) D. H. Wang, W. C. Goh, M. Ning, and C. K. Ong, *Appl. Phys. Lett.* **88**, 212907 (2006).
- 23) K. Ueda, H. Tabata, and T. Kawai, *Appl. Phys. Lett.* **75**, 555 (1999).
- 24) B. Xu, K. B. Yin, J. Lin, Y. D. Xia, X. G. Wan, J. Yin, X. J. Bai, J. Du, and Z. G. Liu, *Phys. Rev. B* **79**, 134109 (2009).
- 25) D. G. Barrionuevo, S. P. Singh, R. S. Katiyar, and M. S. Tomar, *MRS Proc.* **1256**, 1256-N06-47 (2010).
- 26) H. Hojo, R. Kawabe, H. Yamamoto, K. Mibu, and M. Azuma, 1st Semin. Ferroic-Ordering and Their Manipulation, 2016, D-1.
- 27) S. Yoshimura, Y. Sugawara, G. Egawa, and H. Saito, *J. Magn. Soc. Jpn.* **42**, 11 (2018).
- 28) S. Yoshimura, H. Kobayashi, G. Egawa, H. Saito, and S. Ishida, *J. Appl. Phys.* **109**, 07B751 (2011).
- 29) D. R. Pellemounter, D. J. Christie, and B. D. Fries, 57th Annu. Technical Conf. Proc., 2014, p. 183.
- 30) Y. Takeda, S. Yoshimura, M. Takano, H. Asano, and M. Matsui, *J. Appl. Phys.* **101**, 09J514 (2007).



**Satoru Yoshimura** received his Bachelor of Technology (Tohoku University, 1998), Master of Technology (Tohoku University, 1999), and Doctor of Technology (Tohoku University, 2002) degrees. He became a JSPS Research Fellow at the Graduate School of Engineering, Tohoku University (2001), a Research Associate at the Graduate School of Engineering, Nagoya University (2005), an Assistant Professor at the Graduate School of Information Science and Electrical Engineering, Kyushu University (2007), an Associate Professor at the Research Center for Engineering Science, Akita University (2008), and a PRESTO Researcher of JST Strategic Basic Research Programs (2015). His research focuses on the development of electric field-driven magnetic devices with highly functional magnetic thin films.



**Munusamy Kuppan** received his Bachelor of Science (Thiruvalluvar University, 2007), Master of Science (Thiruvalluvar University, 2009), Master of Philosophy (University of Madras, 2011), and Doctor of Philosophy (VIT University, 2015) degrees. He became a Research Assistant at the Centre for Crystal Growth, VIT University (2016), and a Postdoctoral fellow at the Regional Innovation Center, Akita University (2017). His research focuses on the search and fabrication of highly functional magnetic thin films and their applications.